JOURNAL OF Materials CHEMISTRY

Syntheses of mesoporous zirconia with anionic surfactants

G. Pacheco,[a†] E. Zhao,[a] A. Garcia,[c] A. Sklyarov[b] and J. J. Fripiat*[a]

[a]*Department of Chemistry and Laboratory for Surface Studies and* [b]*Advanced Analysis Facility, University of Wisconsin-Milwaukee, P.O. Box 413, Milwaukee, WI 53211, USA*

[c]*Materials Department, Instituto Polytechnico Nacional, Zacatenco, Lindavista, CP 07300, Mexico, DF, Mexico*

Synthesis of mesoporous zirconia has been performed by slowly hydrolyzing zirconium propoxide in the presence of anionic surfactants: dodecyl phosphate or sulfate (P_{12} and Sf_{12}) and hexadecyl sulfonate (So_{16}). *t*-Plot surface areas $>400\ m^2\ g^{-1}$ and diffraction lines corresponding to spacings near 45 Å were measured for solids outgassed at 140–150 °C. This treatment does not remove the surfactant. After calcination in air at 500 °C and combustion of the surfactant the spacing increases to *ca.* 70 Å and the mesoporous volume is reduced by a factor of about 2, whereas the pore wall material crystallizes in the tetragonal phase. A schematic model in which the surfactant is a scaffold component is suggested in order to explain these results. It is very different from the templating mechanisms reported for zirconia by others. The high resolution electron microscopic study reveals the presence of a disorganized network of polygonal pores in the solids obtained through the mediation of surfactant. It is suggested that the chemistry of the hydrolysis solution is instrumental in the organization of the pore structure and in determining the thickness of the walls. In agreement with others, the fixation of PO_4 or SO_4 in the walls may help to preserve the porous structure.

The success of Mobil scientists in the surfactant-assisted synthesis of mesoporous molecular sieves[1,2] with hexagonal (MCM-41) or cubic (MCM-48) ordering of the pore system has been followed by an enormous amount of research worldwide. An array of cationic surfactants (such as quaternary alkylammonium) with chains containing, typically, twelve carbon atoms interact with an inorganic anionic or cationic oligomer (or polymer) to form a solid in which small-angle powder X-ray diffraction (PXRD) reveals the existence of an ordered system of pores. Moreover, in the silicate systems, this order is maintained after the removal of the surfactant, yielding mesoporous systems[3] and specific surface areas in the order of $1000\ m^2\ g^{-1}$.

The basic principles of these syntheses have been reviewed by Huo *et al.*[4] They have distinguished the interaction between cationic or anionic surfactant with cationic or anionic metal oligomers, or between organic and inorganic species with similar charge *via* a counter ion, on the basis of studies involving a large variety of metals other than silicon. Three kinds of structures have been characterized by their PXRD patterns, namely, hexagonal, lamellar and cubic. Usually the higher spacing is easily observed between 2 and 4° 2Θ, whereas the other Bragg reflections, on which the differentiation between the structures is based, have a lower intensity. Removal of the surfactant does not necessarily keep the hexagonal or cubic structure intact, as desirable for producing high area solids.

The synthesis of titanium[5] and of zirconium[6] partially substituted mesoporous silica has been attempted successfully to circumvent the difficulty of preparing stable mesoporous titania or zirconia. However, hexagonally packed transition-metal mesoporous molecular sieves of pure Ti or Ta oxide have been synthesized by Antonelli and Ying.[7,8]

In all these examples, the mechanism of synthesis is undoubtedly *via* the formation of an organic template coated with the inorganic species, as recently reviewed by Raman, Anderson and Brinker.[9] Many variants exist, but, fundamentally, the size of the pores and their distribution is primarily fixed by the templates. The removal of the template creates pores available to N_2, exposing a large surface area. The ordering of the initial pore structure is preserved to a variable extent, depending upon the severity of the removal treatment.

A scaffolding rather than a templating mechanism has been suggested by Hudson and Knowles,[10] who were the first, as far as we are aware, to have prepared mesoporous ZrO_2 with cationic surfactants (alkyltrimethylammonium). The surfactant/Zr ratio was around 0.2. Again, the porosity (to N_2) appears after removal of the surfactant (in this case, by calcination at 500 °C), but the pore ordering which does not exist in the presence of the templates appears after its removal. The experimental observations on which this conclusion is based are the absence of a relationship between the *d*-spacing and the chain length before calcination and its appearance after calcination.

The mechanism suggested by Hudson and Knowles is very different from the templating process, even if the final resulting materials show many similarities. First, the positively charged zirconium hydrogel precipitated at pH [isoelectric point (i.e.p.) is between 6 and 8] is converted into a cation exchanger by raising the pH to 11.5 by aqueous ammonia. The cationic surfactant is fixed by the hydrogel with NH_4^+ being released.

The reduction of the surface tension of the pore water by the surfactant prevents the aggregation of hydrated ZrO_2 particles. There is some ordering of these particles revealed by a broad small-angle PXRD, the position of which is primarily a function of hydration.

The loss of water during subsequent drying or calcination results in the shrinkage of the gel and increased interaction between the alkyl chains anchored to the ZrO_2 surface. The increased temperature permits the condensation between the gel particles. This creates a porous network in which the organic residue burns at *ca.* 400 °C. Now the scale of ordering is determined by the chain length. As also outlined by Hudson and Knowles,[10] the pore diameter at the maximum of the distribution of the pore volume does not necessarily scale like the small-angle PXRD reflection.

We have extensively summarized this work because, as shown later, our results obtained with anionic surfactant can be described in a similar but not identical matter.

It should not be concluded that the templating mechanism is not possible for the hydrous zirconium oxide. Starting from

†On leave of absence from the Instituto Polytechnico Nacional, Mexico D.F.

Zr sulfate or propoxide and using alkyltrimethylammonium surfactants as templates, Schüth[11] and Ciesla *et al.*[12] have obtained a hexagonal mesoporous zirconia of a quality corresponding to that of the silica analogue. Reddy *et al.*[13] obtained either hexagonal or lamellar phases of templated zirconia using either quaternary ammonium surfactants or a solution of acidified primary alkylamine, respectively. A genuine templating mechanism for ZrO_2 seems to require tetraalkylammonium cations with chain lengths ideally larger than C_{12}. Also, it is interesting to note that sulfating and/or phosphating the ZrO_2 gel enhances the crystallinity of the solid before calcination.[12,13] The work of Reddy *et al.*[13] illustrates a curious aspect of the preparation of mesoporous zirconia, namely, the relatively weak influence of the surfactant to ZrO_2 ratios. Similar *d*-spacings (hexagonal phase) are obtained with ratios as different as 0.13 and 1.08. Moreover, Reddy *et al.*[13] and Ciesla *et al.*[12] disagree on the effect of calcination at *ca.* 500 °C, the latter showing that the small-angle PXRD peak and the porosity survive calcination.

For the preparation of mesoporous ZrO_2, Huang *et al.*[14] have used an acidified primary (C_{16}) alkylamine which is easily removed by ethanolic extraction of the precursor. The extracted sample or samples sulfated with H_2SO_4, after synthesis, were calcined up to 650 °C. The small-angle PXRD consists of a broad reflection which remains at about the same spacing (*ca.* 41 Å) as the calcination temperature is increased from 110 to 400 °C; it disappears at 500 °C. Accordingly, the porosity disappears after calcination at 300 °C. The sulfated samples retain their porosity and the small-angle scattering peak up to 600–700 °C. Huang *et al.*[14] point out the difference between sulfated zirconia, hydrolyzed with NH_3 and sulfated, which has a very low mesoporosity, and the sulfated mesoporous zirconia, obtained using alkylamine.

Neutral primary amine surfactants were especially studied by Tanev and Pinnavaia[15] in the synthesis of mesoporous silica. They consider that the main interaction is a weak hydrogen bonding between the surfactant head group and the neutral inorganic precursor. They outline the large increase of the ratio of textural to framework pore volume, using a neutral instead of a cationic surfactant with the same chain length. The scattering domains are also smaller with neutral surfactant and the variation of the position of the single small-angle PXRD peak does not scale as the chain length. Interestingly, a more crosslinked SiO_2 framework is observed with the neutral than with the cationic surfactant, as revealed by the ^{29}Si MAS NMR spectroscopy.

The formation of 'ordered' walls has not drawn much attention, except in the work of Huang *et al.*[14] The general observation is of the loss of small-range ordering upon crystallization. Accordingly, there is a loss or collapse of the porous structure and a decrease in the surface area. Assuming that the repeated distance between cavities within the mesoporous solid and the thickness of the walls are known, it would be of prime interest to correlate these parameters with recrystallization, since the stability of tetragonal ZrO_2 appears to be driven by particle size.[16] Metastable cubic ZrO_2 with a particle size of *ca.* 90 Å has been observed up to 300 °C using a Zr alkoxide as precursor.

From a simple thermodynamic treatment proposed by Garvie[16] and numerical parameters used by Aita *et al.*,[17,18] it can be shown that at 500 °C particles with diameters larger than 160 Å undergo a tetragonal–monoclinic transformation.

Recently, we have reported[19] on the synthesis of mesoporous zirconia using monodecyl sulfate or phosphate. As far as we know, such a synthesis had not been achieved at the time that paper was submitted. However, shortly after, the synthesis of sulfated mesoporous zirconia mediated by lauryl sulfate in alkaline solution was described.[20] Contrary to our results, no small-angle PXRD reflection was observed in the presence or absence of surfactant, but pores in the 20–30 Å range developed a BET surface area of *ca.* 400 $m^2\ g^{-1}$.

In our work the source of zirconium was a 70% m/m solution of Zr propoxide in propan-1-ol. The two 'straight alkyl chain surfactants' $C_{12}H_{25}OP(OH)_2$ ($M=266$), abbreviated P_{12} and $C_{12}H_{25}OSO_3Na$ ($M=288$), abbreviated Sf_{12}, were acidified and the hydrolysis was carried out by slowly adding the propanolic Zr alkoxide solution to the surfactant solution[5] or adding the surfactant (s) to the propanolic Zr alkoxide solution until the molar ratio s/Zr was 0.16.

After drying at 140 °C with no surfactant removal, low-angle PXRD showed a diffraction line corresponding to a spacing of *ca.* 47 Å, while the N_2 adsorption–desorption isotherms exhibited the typical shape expected for mesoporous solids.[18] The *t*-plot surface area was *ca.* 500 $m^2\ g^{-1}$. A network of poorly organized pseudo-hexagonal pores was observed by high resolution transmission electron microscopy (HRTEM). The Gaussian distribution of pore diameters showed a maximum at *ca.* 44 Å. Thus, there was a qualitative agreement between the position of the low-angle PXRD peak, the porosity and the HRTEM observations.

The present study constitutes the continuation of these preliminary experiments.

Essentially, we tried to rationalize the preparation procedures. The basic ideas have been (i) to operate at low pH, in order to facilitate the interaction between the 'nascent' zirconia, or zirconia 'oligomers', as we will call them, and the surfactant, and (ii) to slow the hydrolysis reaction. More work is necessary, especially in the 'ageing' and washing processes as well as in the 'high' temperature treatments ($\geqslant 500$ °C) to optimize the mesoporous characteristic and to understand the synthesis mechanism in a more fundamental way. So far, the latter point had not been our main goal.

Experimental

Reagents

The following surfactants have been used in this work: Fisher Scientific: Na lauryl sulfate, ($S_{529-500}$, Lot 961958), $CH_3(CH_2)_{10}CH_2OSO_3Na$ (Sf_{12}); the Sf_{12} aqueous solution contained 3.5×10^{-3} mol surfactant per 30 ml. Acros: 1-hexadecyl sulfonic acid sodium salt, (41139-0250, Lot A13000), $CH_3(CH_2)_{14}CH_2OSO_2Na$ (So_{16}); the So_{16} aqueous solution contained 3.1×10^{-3} mol surfactant per 30 ml. Alfa: monododecyl phosphate (2627–35–2, Lot 602624), $(C_{12}H_{25}O)PO(OH)_2$ (P_{12}); the P_{12} aqueous solution contained 3.8×10^{-3} mol surfactant per 30 ml. The source of zirconium was a 70 mass% solution of zirconium propoxide in propan-1-ol (Aldrich: 33,397-2, Lot 05201 KQ), abbreviated as Zr prop. The Zr prop solution contained 21.4×10^{-3} mol propoxide per 10 ml.

Preparation procedure

The procedure is schematized in Table 1 where the results of the chemical analysis (%C, H) on the solids dried at 140 °C are also presented.

In the first step, 10 ml of the Zr prop solution were placed in a glass reactor at 0 °C and using an automatic burette, the solution of surfactant was added at the rate of 6 ml h^{-1} upon stirring. A dry N_2 flow of 50 ml min^{-1} prevented the spontaneous hydrolysis of Zr prop upon contact with moisture. This precaution was necessary when, in variant procedures, 10 ml Zr prop were injected over 5 h into the cooled surfactant solution. Hydrolysis blocks the liquid in the automatic burette needle when a flow of dry N_2 is not used. The order of introduction (column 2, Table 1) indicates what reagent is introduced first in the reactor.

Thus, the first step of the preparation is a slow hydrolysis of Zr prop, in the presence of a selected surfactant, dissolved in a mixture of water and propan-1-ol.

When the Zr prop solution is added first, the hydrolysis is carried out initially in the presence of a large excess of Zr

Table 1 Preparation and chemical analysis

sample	order of addition	pH initial–final	acid used	%C	%H	mass% loss/100 (500 °C)	%C after outgassing[a]
Sf_{12} (5)	S_{12} soln.	2–6	HCl	9.90	3.05	0.302	10.5
Sf_{12} (8)	S_{12} soln.	2–7.5	H_2SO_4	7.79	2.45	0.248	8.7
So_{16} (1)	$Zr(OPr)_4$	2–7.0	HCl	13.36	3.26	0.324	
So_{16} (2)	S_{16} soln.	2–7.0[b]	HCl	11.21	2.97	0.240	
So_{16} (3)	S_{16} soln.	2–7.3[b]	H_2SO_4	6.99	2.20	0.152	
P_{12} (1)	$Zr(OPr)_4$	1–3.0	HCl	3.37	1.98	0.169	
P_{12} (2)	P_{12} soln.	1–3.0	HCl	2.05	1.96	0.146	
P_{12} (4)	P_{12} soln.	2–3.8	H_3PO_4	9.68	3.27	0.233	11
P_{12} (5)	P_{12} soln.	2–4.7[d]	HCl	2.76	1.84	0.124	
P_{12}(6)	P_{12} soln.	1.8–2.7	H_3PO_4	2.24	1.95	0.123	2.3
Zr prop	propan-1-ol–water	2–7.0	HCl	0.66[d]	1.17	0.091	

[a]Carbon in some selected samples after outgassing at 150 °C overnight prior to the N_2 adsorption measurement. [b]Volume propan-1-ol/volume propan-1-ol + water = 43%; [c]30% and [d]30%. All others 10%, corresponding to the propan-1-ol content of the Zr prop propanolic solution. [e]Carbon arises from adsorbed propan-1-ol.

propoxide and propan-1-ol. When the surfactant solution is added first, the hydrolysis proceeds initially in a large excess of surfactant. In all cases, the final molar ratio surfactant/Zr (s/Zr) was *ca.* 0.16.

The pH of the surfactant/water–propan-1-ol solution was adjusted initially at the values shown in Table 1, using either HCl, H_2SO_4 or H_3PO_4.

The hydrolysis step was followed immediately by an ageing step where the suspension of hydrolyzed zirconia in the surfactant solution was stirred for 12 h at 40 °C. The final pH was then measured (Table 1). At the end of the first ageing step, the solid was removed from the reactor and transferred in a hydrothermal stainless steel pressure tube containing 5–10 ml water. The tube was heated at 140 °C for 48 h with continuous end-over-end rotation. After cooling, the solid was removed from the tube and transferred into a centrifuge tube with *ca.* 20 ml water and washed once more by centrifugation with 20 ml water. It was then dried at 140 °C for 2 h. Part of it was then calcined in air at 500 °C for 12 h, the heating rate being 250 °C h^{-1}.

The physical and chemical characterizations were performed on the solids dried at 140 °C or calcined at 500 °C. The samples are designated according to the used surfactant (*e.g.* Sf_{12}), the particularities of the procedure, listed in Table 1 [*e.g.* Sf_{12} (5)], and the final thermal treatment [*e.g.* Sf_{12} (5) 140 °C]. For comparison, Zr prop was hydrolyzed under identical conditions in the presence of propan-1-ol in 30 ml of water at pH 2 without adding surfactant.

Chemical characterization

The C and H contents of the sample dried at 140 °C were determined using a Carlo Erba CHN analyzer and are listed in Table 1, the mass% values being referred to the sample calcined at 140 °C. In order to interpret these results, it is assumed that the Zr propoxide was completely hydrolyzed and that the resulting propan-1-ol, or the propan-1-ol added to the surfactant solution and the excess surfactant were washed out by the two centrifugations carried out before drying. Drying at 140 °C should remove weakly adsorbed propan-1-ol and water. Hence, the carbon content could be assigned to the remaining surfactant to a first approximation. From the analysis of the C content after outgassing at 150 °C prior to the measurements of the N_2 adsorption–desorption isotherm, it can be concluded that no surfactant has been removed by this treatment.

There was always an excess of hydrogen with respect to the hydrogen contained in the surfactant. This excess was assigned to adsorbed water. It decreases to *ca.* zero upon outgassing. No carbon was detected after calcination in air at 500 °C, as expected.

The residual sulfur [in Sf_{12} (8)] or phosphorus [in P_{12} (4)] were detected by ESCA. Within a relative high margin of uncertainty, the atomic ratios of elemental sulfur/Zr or elemental phosphate/Zr were of the same order of magnitude as those s/Zr obtained from chemical analysis. Interestingly, the O 1s peak in P_{12} (4) seems to contain only one component with $E_b = 530.5$ eV, while the O 1s peak in Sf_{12} (8) apparently contained two contributions at 529.2 and at 530.5 eV, respectively.

Physical characterization

(a) PXRD. Low-angle PXRD between 0.8 and 10° 2Θ was obtained with a Scintag Θ–Θ X-ray diffractometer (Cu-Kα) with the following set of slits 0.5, 0.3, 0.2 and 0.07°. The scanning rate was 1° min^{-1} and a solid state detector was used. Under these conditions a diffraction peak corresponding to spacing up to *ca.* 90 Å can still be observed. For medium-angle PXRD (2–70°), the slits were 3, 2, 0.5 and 0.3°.

(b) Adsorption isotherms. N_2 adsorption and desorption isotherms were obtained with an automated physisorption instrument operated in a static mode (Omnisorp 100, Coulter Co.). Between 20 to 30 Torr increments were used with a total instrumental time of about 16 h per isotherm. The desorption isotherms were analyzed using the BJH[21] algorithm for mesoporosity. All measurements were performed after outgassing the sample at 150 °C under vacuum, down to a residual pressure better than 10^{-4} Torr.

(c) SEM. The particle morphology was examined by scanning electron microscopy with a TOPCON ABT-32 instrument equipped with an EDX microprobe analyzer. The Au–Pd deposition was applied using a magnetron sputtering system from Plasma Sciences Inc. All measurements were conducted at 10 kV.

(d) HRTEM. Some materials were examined with high resolution transmission electron microscopy (HRTEM) at 200 kV. The samples were supported on a collodium film and a carbon grid. As shown later, disorganized networks of pseudo-hexagonal pores were observed in which approximate measurements of sizes were carried out. Attempts were also made to observe diffraction patterns.

(e) ^{31}P MAS NMR. The spectra were measured in a field of 11.7 T in the P_{12} (4) solid dried at 150 °C or calcined at 500 °C in air.

Results and model

The most striking result obtained in this work is the development of a large surface area and mesoporous volume in solids

dried at 140 °C in air or at 150 °C in vacuum, containing variable and relatively large amounts of surfactants, between 0.14 and 0.69 mmol per g of solid (Table 2).

All the solids described in the literature, as reviewed in the introductory section, required the removal of the surfactant by chemical extraction, or calcination, before exhibiting the mesoporosity. This fact, alone, already indicates that we are not dealing with a templating mechanism. Rather we favor a scaffolding mechanism. This term, coined by Hudson and Knowles[10] is not going to be used in exactly the same sense, but describes a mechanism having similarities to theirs, and we will present a schematic scaffolding model.

However, before continuing, it is appropriate to discuss the set of physical characteristics shown in Table 3. The porous volume V_o is obtained from the type IV desorption isotherms[22] and expressed in ml liquid N_2 in cylindrical pores with a pseudo-diameter between 15 and 100 Å. Below 15 Å, the porous volume is negligible, whereas above 100 Å the average (0.04 ml g^{-1}) is between 0.02 ml [P_{12} (5) 140 °C] and 0.09 ml [P_{12} (4) 140 °C].

The small-angle PXRD also calls for some comment. In this work, we have never observed more than a broad and weak peak with a maximum in the range listed in Table 3. As far as the peak intensity is concerned, it is difficult to make comparisons with results by others, since no indication about the intensity was found in the references reviewed. The broadness is comparable to that obtained by others when no reflection other than the basal one is observed. The spacing corresponding to the small-angle PXRD reflection, apparently, is independent of the chain length after drying at 140 °C or calcination at 500 °C.

The first step in formation of the gel is the aggregation in a tail-to-tail manner of the surfactant molecules, each having fixed on their polar head a positively charged zirconia oligomer made from between *ca.* 5 to 15 ZrO_2 units, as suggested by the chemical data in Table 2. The link between the polar head and the surfactant at the pH of synthesis (Table 1) is probably hydrogen bonding like that suggested for the neutral surfactant. The 'elementary particle' would have the structure shown in Fig. 1A. Such particles would associate through condensation of ZrO_2 oligomers in a sheet having a thickness smaller than the chain length, which is *ca.* 15 Å for Sf_{12} and P_{12} and 20 Å for So_{16}. Then, under the influence of the van der Waals forces balancing the electrostatic repulsion, the sheets would associate in tactoids containing the porous volume.[23] The cubic arrangement in Fig. 1B is chosen for the sake of simplicity, but any polygon would suffice. It allows simple calculations leading to an equivalent pore 'diameter' ($S-t$), while the periodicity is given by the small-angle PXRD reflection. If the gel consists of the repetition of n subunits along the x and y axes, while L is the extension along the z axis, then the volume of matter, V_m, is

$$V_m = L[(S+t)^2-(S-t)^2]n \quad (1)$$

and the void volume, V_o, is

$$V_o = L(S-t)^2n \quad (2)$$

L is probably much smaller than nS. From eqn. (1) and (2) and the definition of the density ρ we have:

$$\rho V_o = (r^2-1)^{-1} \quad (3)$$

where

$$r^2 = \left(\frac{S+t}{S-t}\right) = (1+(\rho V_o)^{-1}) > 1$$

and where unambiguously, in the frame of the model, the wall

Table 2 Chemical data

sample	mmol s/g (140 °C)[a]	s/Zr	s/Zr (soln.)
Sf_{12} (5)	0.69	0.110	0.164
Sf_{12} (8)	0.54	0.104	0.164
So_{16} (1)	0.69	0.153	0.145
So_{16} (2)	0.58	0.112	0.145
So_{16} (3)	0.36	0.060	0.145
P_{12} (2)	0.14	0.023	0.178
P_{12} (4)	0.67	0.124	0.178
P_{12} (5)	0.19	0.030	0.178
P_{12} (6)	0.15	0.023	0.178
Zr[b]	0.18	0.017	—

[a]Millimole surfactant (s) per g of solid dried at 140 °C or per zirconium in the solid. [b]mmol propan-1-ol g^{-1} (140 °C) or propan-1-ol/Zr molar ratio.

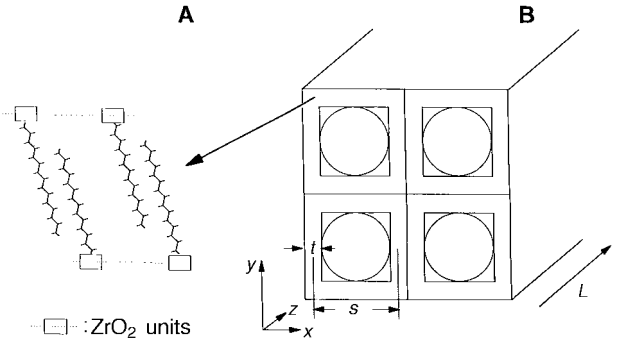

Fig. 1 Schematic model illustrating the scaffolding mechanism: A, the primary particle or scaffold component; B, porous structure

Table 3 Physical characterization: total volume, porous volume and position of the low-angle PXRD peak

	samples dried at 140 °C				samples calcined at 500 °C				
sample	V_o[b]/ml g^{-1} ($15 \leqslant \phi \leqslant 100$)	V_o/V_t[c] (%)	t-plot/ m^2 g^{-1}	PXRD reflection S/Å	V_o[b]/ml g^{-1} ($15 \leqslant \phi \leqslant 100$	V_o/V_t (%)	t-plot/ m^2 g^{-1}	V_{red}[a] (%)	PXRD reflection S/Å
Sf_{12} (5)	0.266	89	220	47	0.092	76	78	65	54.4
Sf_{12} (8)	0.404	85	335	32	0.125	72	116	69	64.5
So_{16} (1)	0.120	65	93	33.7	0.130	68	95	*ca.* 0	72.4
So_{16} (2)	0.288	85	247	46.5	0.131	82	115	54	82.5
So_{16} (3)	0.562	84	452	60	0.140	71	120	75	91.0
P_{12} (1)	0.375	71	291	47	0.254	68	200	32	85.0
P_{12} (2)	0.188	84	155	41	0.110	84	87	41	68.8
P_{12} (4)	0.433	80	355	46	0.263	76	227	39	69.0
P_{12} (5)	0.439	96	384	46.5	0.118	85	103	73	48.1
P_{12}(6)	0.611	91.6	455	80	0.471	91.6	380	23	66.7
Zr prop	0.51	93.2	420	45.5	0.170	84	54.5	—	

[a]Reduction factor, $(V_{140}-V_{500})/V_{140}$. [b]Porous volume with diameter ϕ between 15 and 100 A. [c]V_t is the total meso- and macro-pore volume.

thickness t is

$$t = S\left(\frac{r-1}{r+1}\right) < S \qquad (4)$$

The density ρ is approximated by the sum of the mass of the inorganic and inorganic (Zr oligomer) constituents divided by the sum of their volume. The density of the organic part is assumed to be 1 g cm^{-3}, whereas that of the Zr oligomer was taken equal to 3.2 g cm^{-3} before calcination, namely, the density reported for amorphous zirconia.[24] After calcination the density is similar to that of tetragonal zirconia, *ca.* 5.6 g cm^{-3}.[24]

Using the mesoporous volume V_o, and the PXRD basal distance S shown in Table 3, the thickness of the walls and the apparent pore diameter $(S-t)$ reported in Table 4, were obtained.

The basal distance does not change much in the samples dried at 140 °C. Out of ten samples, seven exhibit an averaged reflection at *ca.* 45 Å. After calcination, 5 out of 10 have reflections between 60 and 80 Å. Thus, the variability in the porous volume is attributable in the first approximation to the thickness or to the density. The lower the density, the larger is the thickness. The larger the ratio s/Zr is, the lower the density. Sample P_{12} (6) prepared at the lowest pH (H_3PO_4) has the highest mesoporous volume and, unexpectedly, the highest PXRD reflection (80 Å) after drying at 140 °C. These results were reproducible.

Fig. 2–4 illustrate the type of small-angle PXRD reflections and N_2 adsorption–desorption isotherms obtained with surfactants.

The model helps to explain much of the experimental data. First, there is the observation (Fig. 5) that the slow hydrolysis of the zirconium propoxide (Zr prop, Table 1) in a propanolic aqueous solution leads to a gel which shows a relatively intense PXRD basal reflection and a large mesoporous volume when dried at 140 °C. This observation suggests that the aggregation of the Zr oligomer plays an important role in the formation of the sheet (Fig. 1B). The thickness of the wall is also the smallest in Zr prop dried at 140 °C, and after calcination at 500 °C the small-angle PXRD is no longer observed. The surfactant and eventually the propan-1-ol interact with the Zr oligomer by formation of hydrogen bonds, resulting in production of the primary particles which eventually form the sheet.

The elimination of the water–propan-1-ol mixture upon drying the gel does not destroy the delicate architecture shown in Fig. 1B. Upon increasing the temperature to 500 °C and ultimately burning the surfactant, further condensation of the ZrO_2 oligomers occurs, resulting in a shrinkage of the walls and the sintering of adjacent walls (Fig. 1B).

Table 4 Calculated pore diameter and thickness

sample (500 °C)	pore diameter (140 °C)/ Å	wall thickness (140 °C)/ Å	$\langle\rho\rangle^a$/ g cm^{-3} (140 °C)	pore diameter (500 °C)/ Å	wall thickness (500 °C)/ Å
Sf_{12} (5)	34.5	12.5	1.9	40.1	14.3
Sf_{12} (8)	25.7	6.3	2.04	50.4	14.1
So_{16} (1)	20	13.5	1.85	57	15.4
So_{16} (2)	35.3	11.2	2.07	65	17.5
So_{16} (3)	52.5	8.5	2.35	72.6	18.4
P_{12} (1)	38.1	8.95	2.29	73.8	11.2
P_{12} (2)	29.3	11.7	2.38	52.5	16.3
P_{12} (4)	37.6	8.4	2.11	60.1	8.9
P_{12} (5)	39.4	7.6	2.47	37.2	10.9
P_{12} (6)	70.0	10.1	2.47	61.4	5.35
Zr prop	39.2	6.3	2.62	—	—

[a]The density after calcination at 500 °C is that of tetragonal zirconia (5.6 g cm^{-3}) and is thus constant. After drying at 140 °C, ρ depends upon the mass of the organic fraction and the mass of the inorganic fraction. The density of the latter is assumed to be 3.12 g cm^{-3}.[22]

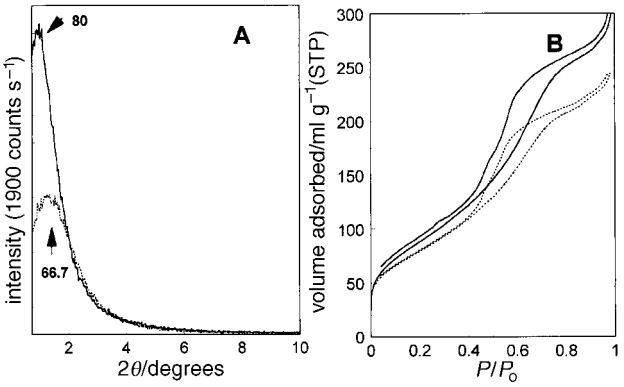

Fig. 2 A, Low-angle PXRD reflections of the solid obtained in the presence of P_{12}. See P_{12} (6), Tables 1 and 2 and text for details. Top: solid line, solid dried at 140 °C. Bottom: dashed line, solid calcined at 500 °C. The number of counts per second indicated between parentheses, corresponds to the maximum intensity. B, N_2 adsorption–desorption isotherms at −196 °C on P_{12} (6) 140 °C (solid line) or calcined at 500 °C (broken line).

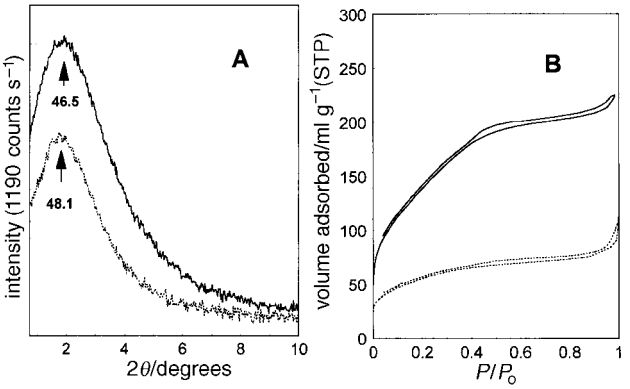

Fig. 3 Sample P_{12} (5), Table 1. See Fig. 2 caption for key.

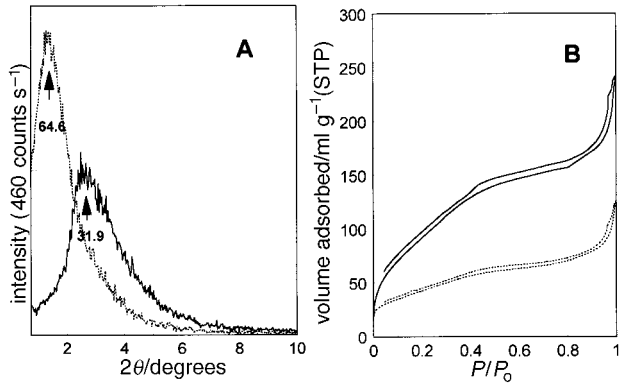

Fig. 4 Sample Sf_{12} (8), Table 1. See Fig. 2 caption for key.

The net results are (i) an increase in the basal reflection and a decrease in the mesoporous volume (Table 3), despite an increase in the calculated pore diameter, and (ii) a noticeable increase in the wall thickness (Table 4). These observations which completely contradict what has been reported for templated materials, are easily understood when considering the increase in density from *ca.* 2 g cm^{-3} in the material dried at 140 °C to 5.6 g cm^{-3} in the material calcined at 500 °C [eqn. (3) and (4)].

The transformation of quasi-amorphous walls into crystallized walls is evidenced by the PXRD reflections at 'high' angle ($2\Theta > 10°$) shown in Fig. 6. For the samples prepared in

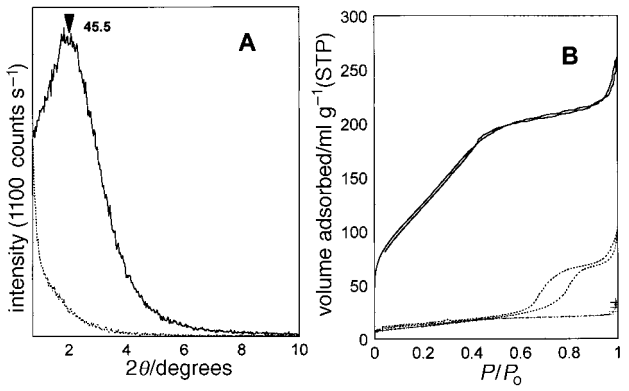

Fig. 5 Sample Zr prop (see Tables 1 and 2). See Fig. 2 caption for key. In (B) the crosses represent the adsorption isotherm obtained for a sample of Zr propoxide hydrolyzed at pH 7 in an excess of water at room temperature and calcined at 250 °C.

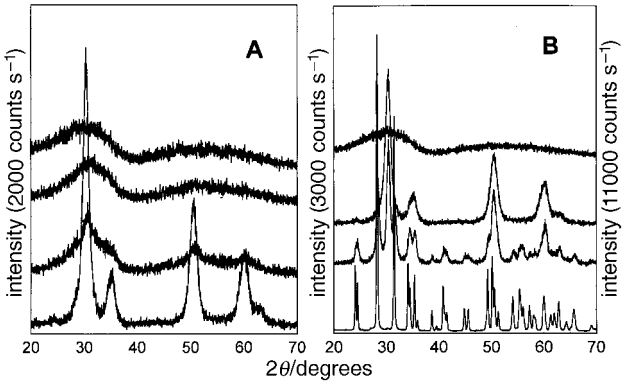

Fig. 6 Examples of PXRD patterns in the 2Θ 20–70° region. A, Samples dried at 140 °C. From top to bottom: samples P_{12} (4), So_{16} (3), Zr prop and tetragonal ZrO_2. B, Samples calcined at 500 °C. From top to bottom: samples P_{12} (4), So_{16} (3), Zr prop and monoclinic ZrO_2 (baddeleyite). All other samples dried at 140 °C look like P_{12} (4) or So_{16} (3) in A. All other samples calcined at 500 °C look like So_{16} (3) in B (tetragonal zirconia). Thus, quasi-amorphous P_{12} (4) in B is an exception. A mixture of monoclinic and tetragonal zirconia is observed in Zr prop (500 °C).

the presence of surfactant and dried at 140 °C, Fig. 6A, two very broad and diffuse reflections are observed, the most intense being at *ca.* 2.90 Å.

The solid obtained in the absence of surfactant is an exception in the sense that three weak and broad diffraction lines were observed at 2.90, 1.79 and 1.54 Å. Accordingly, weak spots were observed in the electron diffraction diagrams obtained for this sample.

After calcination at 500 °C, all samples prepared with surfactant [except for P_{12} (4) and P_{12} (6)], show the PXRD pattern typical for tetragonal zirconia (Fig. 6B). Thus, in Fig. 6A the broad lines in the sample prepared without surfactant indicate the onset of crystallization into tetragonal zirconia. This sample heated at 500 °C shows a mixture of tetragonal and monoclinic zirconia. This crystallization did not occur in the samples prepared with surfactant and in which mesoporosity subsists after calcination. In our previous study,[19] a similar situation was encountered in a solid prepared differently with Sf_{12}.

In short, the occurrence of monoclinic zirconia is related to the shift of the pore distribution towards a larger pore size. The sintering is delayed to temperatures >500 °C in materials prepared with surfactant.

The HRTEM study performed on So_{16} (3) and on a P_{12} mesoporous zirconia, Zr prop, prepared without surfactant, dried at 140 °C or calcined at 500 °C also supports the model. Disordered aggregates of polygonal holes are observed in the thin region of So_{16} (3) dried at 140 °C, as reported previously for a mesoporous zirconia prepared similarly with P_{12} (5) (Fig. 7). It is suggested that these poorly ordered polygonal holes represent the projection of the schematic model (Fig. 1B) on plane *XY*. In Fig. 8B the overall diameters of the pseudo-hexagons have been fitted by a normalized Gaussian and the actual measurements agree well with those obtained pre-

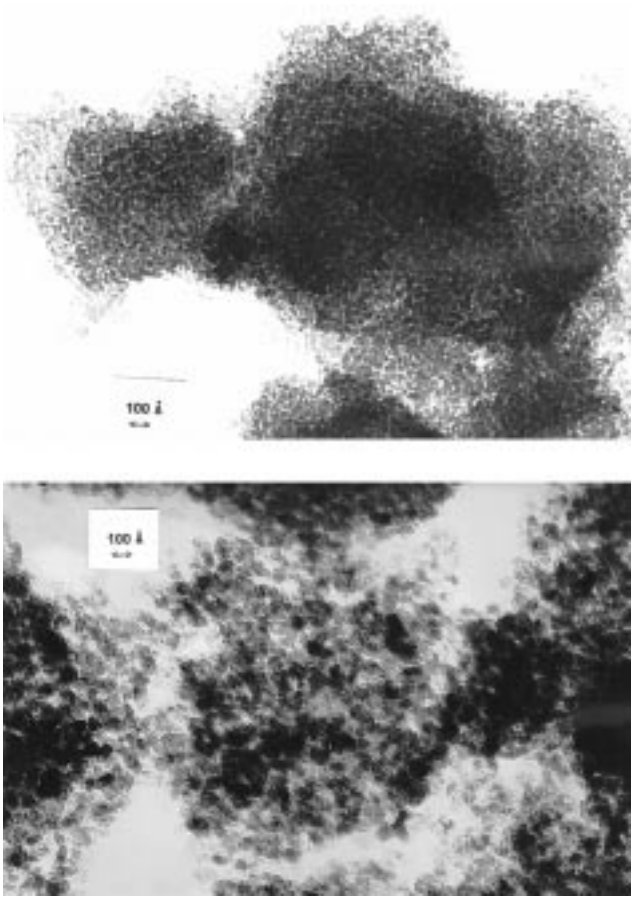

Fig. 7 High resolution transmission electron micrograph picture obtained for So_{16} (3) dried at 140 °C (top), or calcined at 500 °C (bottom). In spite of the disordered aggregation, the polygonal structure depicted in Fig. 1B is clearly visible at the border of the aggregate.

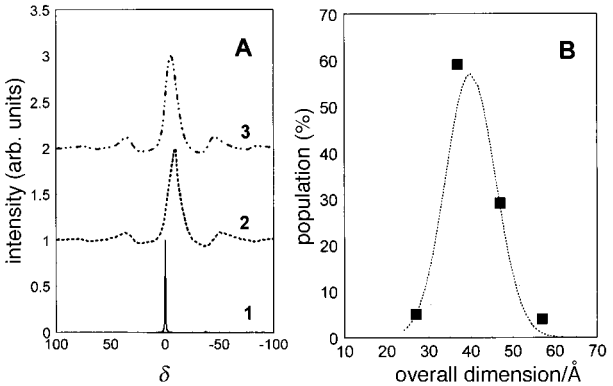

Fig. 8 A, One-pulse ^{31}P MAS NMR spectra in a field of 11.7 T observed for the P_{12} (4) solids dried at 150 °C (3) and 500 °C (2), compared to that of the pure P_{12} surfactant (1). The conditions were as follows: spinning rate 8.5 kHz; 4.5 μs 90° pulse; 10 s relaxation delay; 100 scans; no proton decoupling was used; the chemical shifts of the dried solid samples are referenced to the chemical shift of the pure P_{12} surfactant. B, Gaussian distribution of the overall dimension (Å) of the polygonal holes (hole+walls) measured on the HRTEM picture of sample So_{16} (3) (■) dried at 140 °C, as shown in Fig. 7. □, data published in ref. 19, obtained with a P_{12} surfactant.

viously.[19] The most probable diameter is 40 Å and the width of the Gaussian is 6 Å. In the thicker region of the same picture, the irregularly shaped particles are obviously very porous. In So_{16} (3) heated at 500 °C, the particle size has increased and the contrast is reinforced, as expected, owing to the increase in density accompanying the formation of tetragonal zirconia. Most of the tiny polygonal features observed in the sample dried at 140 °C are no longer observable.

The Zr prop sample dried at 140 °C is composed of porous particles with an overall dimension $\leqslant$50 Å. Heating Zr prop to 500 °C leads to an increase in the particle size to *ca.* 100 Å.

The morphology of secondary structures of several samples dried at 140 °C or calcined at 500 °C have been examined by SEM. Large aggregates (0.1–3 μm) constructed from a collection of polydispersed pseudo-spherical particles, looking like 'sponges' are commonly observed as shown in Fig. 9, similar to examples of morphology shown by Tanev and Pinnavaia[15] [Fig. 3(c)] and obtained for MCM-41 using the $S^+X^-I^+$ procedure. Besides the 'rounded' species, lamellar objects with somewhat sharper edges are also observed. These objects often contain spherical particles inside their structure as observed and reported by Huo *et al.*[25] Note that for So_{16} (3) and P_{12} (5), the calculated pore diameters are 52.5 and 39.4 Å, *i.e.* in the range of the Gaussian distributions shown in Fig. 8B.

Discussion

In commenting on the data presented in Tables 3 and 4, the possible influences of the modes of preparations summarized in Table 1 on the chemical characteristics have been outlined. In order to obtain zirconia with large mesoporous volume, hydrolysis must be carried out at initial pH $\leqslant$2 and slowly, hence, the beneficial effect of lowering the temperature and increasing the proportion of propan-1-ol in solution.

The usual representation of the porosity distribution obtained in calculating (dV_{void}/dR) in the pore diameter domains $>$20 Å (onset of the application of the BJH formalism), as shown in Fig. 10A, illustrates that the limit of the pore-size diameter above which the pore volume no longer increases appreciably is *ca.* 50 Å. After calcination at 500 °C the total pore volume decreases as shown in Table 3, but the relative evolutions are similar. Even in the sample Zr prop dried at 140 °C, prepared without surfactant, the distribution does not differ notably from the others (Fig. 10B). The main difference is observed in Zr prop calcined at 500 °C. In the absence of surfactant, calcination leads to a total redistribution of the porosity (Fig. 10B). The surfactant has a profound effect on the spatial organization of the zirconia oligomers during the hydrolysis, since after a severe thermal treatment such as calcination at 500 °C, the pore size distribution is not dramatically modified, in spite of the formation of tetragonal ZrO_2.

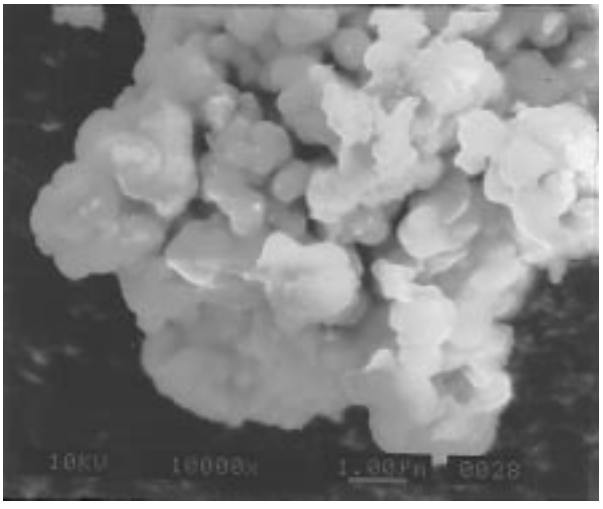

Fig. 9 Typical scanning electron micrograph picture of sample P_{12} (5) dried at 500 °C

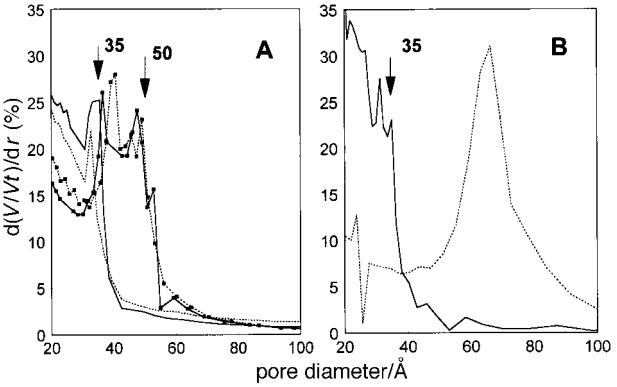

Fig. 10 BJH[21] distribution of mesoporosity *vs.* pore diameter (Å). A: —, So_{16} (3) 140 °C; ■——■, P_{12} (6) 140 °C; ---, So_{16} (3) 500 °C; ■---■, P_{12} (6) 500 °C. B: Zr prop. dried at 140 °C (solid line) or at 500 °C (broken line).

It should be noted that the 'knee' observed in isotherms of type IV attributed to mesoporous solids is at the worst place for obtaining a 'good' pore size distribution. It is outside the range of application of the Horvath–Kawazoe (H–K) algorithm,[26] frequently used without justification beyond 10 Å, *e.g.*, its limit of applicability. It is at the onset of the BJH treatment which applies at pore sizes larger than *ca.* 20 Å. A good illustration of the importance of the P/P_0 range where the 'knee' is observed is found in the comparison of Fig. 5B (between isotherms dried, top; calcined samples, bottom) and the corresponding pore-size distribution in Fig. 10A. In the sample dried at 140 °C, the 'knee' is at P/P_0 between 0.4 and 0.5, while it is between 0.65 and 0.75 in the calcined sample. In the first case, the BJH pore size distribution falls rapidly to zero at an apparent pore diameter near 40 Å, while in the second case a clean maximum is obtained at *ca.* 68 Å. The experimental results suggest that propan-1-ol may also act as a scaffolding reagent, but the mesoporosity is obviously less pronounced than that obtained with an anionic surfactant.

Despite the generally poor quality of the pore size distribution functions, there is a semi-quantitative agreement with the calculated pore diameter (Table 4) and with the Gaussian distribution of the overall dimension of the polygonal, pseudo-hexagonal holes, obtained from HRTEM.

The data reported above for the mesoporous zirconia obtained by the hydrolysis of Zr propoxide carried on in the presence of anionic surfactants are similar to those reported for solids obtained with cationic surfactants. For instance, the BET surface areas (after calcination at 500 °C) obtained by Hudson *et al.*[10] compare well with the *t*-plot areas reported in Table 3. The porous zirconium oxophosphates prepared by Ciesla *et al.*[12] in the presence of hexadecyltrimethylammonium bromide showed PXRD reflections at 41.6 Å. Their pore volume, and ours, were in the order of 0.122 ml g^{-1} after calcination at 500 °C. The s/Zr ratios in the solutions used in ref. 10 and 12 were in the order of 0.5. Owing to solubility limitations the ratios in our case were $<$0.2 and, in the case of So_{16}, propan-1-ol had to be added to lead to dissolution of the surfactant.

Huang *et al.* used acidified hexadecylamine and zirconium propoxide in a ratio of *ca.* 0.3. This procedure gave solids with pore volumes similar to those reported here. In addition, the low-angle PXRD 'peak' gave similar spacing and only one reflection was observed. By contrast, in the preparation procedures using tetraalkylammonium ions, a better resolution was usually achieved which allowed for the observation of

higher order reflections, for instance, the hexagonal {110}, {200}, and {210} reflections in ref. 12.

The cost of the easy removal of the surfactant and of the scaffolding mechanism is, obviously, a much poorer order in the resulting structure.

Another striking difference between the solids obtained with both categories of surfactants and of mechanisms is the effect of calcination on the PXRD reflections. With cationic surfactants the low-angle PXRD shifts towards a higher angle upon calcination at 500 °C, while it shifts towards a lower angle with anionic surfactants, with the exception of P_{12} (6).

The question which should be addressed now is, what are the reasons for a scaffolding rather than a templating mechanism?

Presumably, the first reason to be considered is the strength of the link surfactant–ZrO_2 oligomer. This link is weak and most likely involves hydrogen bonding at low pH, as in this work. However, Tanev and Pinnavaia[15] consider the formation of mesoporous silica with neutral surfactant as a templating mechanism, despite the absence of scaling between chain length and PXRD basal spacing.

A second reason may be found in the use of acid media: the electrostatic repulsion between positively charged oligomers is competing with the condensation reaction favoring the formation of the primary particles, as shown in Fig. 1A. Perhaps, also the addition of H_2SO_4 or H_3PO_4 would favor condensation *vs.* repulsion. ^{31}P MAS NMR spectroscopy supports this idea and Fig. 8A shows spectra for the pure surfactant, the solid dried at 140 °C and the calcined (500 °C) materials. In the solid dried at 140 °C, the chemical shift with respect to that in the surfactant is shifted upfield by −3 ppm, while it is shifted by −8 ppm after calcination at 500 °C. In the latter case, PO_4 was incorporated in the solid wall. In the former case, the shift is due to the interaction with the ZrO_2 oligomer, however more NMR work is needed to attain a fuller picture.

Finally, the last question to address, and the most difficult to answer, concerns the variation observed in the s/Zr ratios (Table 2), for very similar modes of preparation. From experiments, reported or not reported here, the most important parameter in this respect is the pH which, in fact, determines the balance between condensation and repulsion between the Zr oligomers. In turn, the s/Zr ratio determines the density of the solid dried at 140 °C and the magnitude of the effect predicted by eqn. (3) and (4) on the wall thickness.

In the same vein, it is interesting to note that the average wall thicknesses (solids dried at 140 °C) are 9.4, 9.3 and 11.1 Å with the Sf_{12}, P_{12} and So_{16} surfactants, respectively, and that from their length the corresponding average overlappings (thickness/length) are 0.62, 0.63 and 0.56, respectively. The non-scaling of the wall thickness with the chain length is due to different overlapping,

One of us (G. P. M.) wishes to thank COFAA-IPN for a scholarship and the metallurgy department of ESIQIE for the use of the HRTEM. We wish to thank D. S. Hardcastle (AAF) for his valuable help and advice. The financial help of DOE grant DE-FG02-90 ER1430 is gratefully acknowledged.

References

1 C. T. Kresge, M. E. Leonowicz, W. J. Roth, J. C. Vartuli and J. S. Beck, *Nature* (*London*), 1992, **359**, 710.
2 J. S. Beck, J. C. Vartuli, W. J. Roth, M. E. Leonowicz, C. T. Kresge, K. D. Schmitt, C. T-W Chu, D. H. Olson, E. W. Sheppard, S. B. McCullen, J. B. Higgins and J. L. Schlenker, *J. Am. Chem. Soc*., 1992, **116**, 10 836.
3 D. H. Everett, *IUPAC, Division of Physical Chemistry Manual of Symbols and Terminology for Physicochemical Quantities and Units, App. II, Part 1*, Butterworths, London, 1971; mesopores have pore widths in the range of 2–50 nm.
4 Q. Huo, D. L. Margoles, U. Ciesla, D. G. Demuth, P. Feng, T. E. Gier, P. Sieger, A. Firouzi, B. F. Schmelka, F. Schüth and G. D. Stucky, *Chem. Mater*., 1996, **6**, 1176.
5 P. T. Tanev, M. Chibwe and T. J. Pinnavaia, *Nature* (*London*), 1996, **368**, 321.
6 S. A. Bagshaw, E. Prouzet and T. J. Pinnavaia, *Science*, 1995, **269**, 1242.
7 D. M. Antonelli and J. Y. Ying, *Chem. Mater*., 1996, **8**, 874.
8 D. M. Antonelli and J. Y. Ying, *Angew. Chem., Int. Ed. Engl*., 1995, **34**, 2014.
9 N. K. Raman, M. T. Anderson and C. F. Brinker, *Chem. Mater*., 1996, **8**, 1682.
10 M. J. Hudson and J. A. Knowles, *J. Chem. Soc., Chem. Commun.* 1995, 2083.
11 F. Schüth, *Ber. Bunsen-Ges. Phys. Chem*., 1995, **99**, 1306.
12 V. Ciesla, S. Schacht, G. D. Stucky, K. K. Unger and F. Schüth, *Angew. Chem., Int. Ed. Engl*., 1996, **35**, 541.
13 J. S. Reddy, and A. Sayari, *Catal. Lett*., 1996, **38**, 219.
14 Yin-Yan Huang, T. J. McCarthy and W. M. H. Sachtler, *Appl. Catal. A.: General* 1996, **148**, 135.
15 P. T. Tanev and T. J. Pinnavaia, *Chem. Mater*., 1996, **8**, 2068.
16 R. G. Garvie, *J. Phys. Chem*., 1978, **82**, 219. NB: By analogy with others, the PXRD shown in Fig. 6A is assigned to the tetragonal phase. However, since no Rietveld analysis has been performed, confusion with the cubic phase is possible.
17 (*a*) A. Chatterjee, S. K. Pradhan, A. Dakka, M. De and D. Chakravorthy, *J. Mater. Res*., 1996, **9**, 263; (*b*) C. R. Aita, M. D. Wiggins, R. Whig, C. M. Scanlan and M. Gajdardziska-Josifovska, *J. Appl. Phys*., 1994, **79**, 1176.
18 M. Gajdardziska-Josifovska and C. R. Aita, *J. Appl. Phys*., 1994, **79**, 1315.
19 G. Pacheco, E. Zhao, A. Garcia, A. Sklyarov and J. J. Fripiat, *Chem. Commun*., 1997, 491.
20 G. Larsen, E. Lotero, M. Nabity, L. M. Petkovic and D. S. Shobe, *J. Catal*., 1996, **164**, 246.
21 E. P. Barrett, L. G. Joyner and P. H. Halenda, *J. Am. Chem. Soc*., 1951, **13**, 573.
22 S. J. Gregg and K. S. W. Singh, *Adsorption, Surface Area and Porosity*, Academic Press, New York, 1982.
23 H. Van Damme, P. Levitz, J. J. Fripiat, J. F. Alcover, L. Gatineau and F. Bergaya, *Physics of Finely Divided Matter*, ed. N. Boccara and M. Daoud, Springer Verlag, New York, 1986, p. 24. Aggregation of thin platelets: J. F. Lambert, Z.-Q. Deng, J. B. d'Espinose and J. J. Fripiat, *J. Colloid Interface Sci*., 1989, **132**, 336.
24 *Handbook of Chemistry and Physics*, ed. R. C. Weast, The Chemical Rubber Co., Boca Raton, FL, 52nd edn., 1972, p. B156.
25 Q. Huo, J. Feng, F. Schüth and G. D. Stucky, *Chem. Mater*., 1991, **9**, 14.
26 G. Horvath and K. J. J. Kawazoe, *J. Chem. Eng. Jpn*., 1983, **16**, 470.

Paper 7/03819D; *Received* 2*nd June*, 1997